JOURNAL OF AGRICULTURAL AND FOOD CHEMISTRY

Article

pubs.acs.org/JAFC

Silicon and Germanium Nanoparticles with Tailored Surface Chemistry as Novel Inorganic Fiber Brightening Agents

Santanu Deb-Choudhury,*[,†] Sujay Prabakar,[‡] Gail Krsinic,[†] Jolon M. Dyer,[†,§] and Richard D. Tilley[‡]

[†]Protein Quality and Function, AgResearch Lincoln Research Centre, Christchurch 8140, New Zealand

[‡]Victoria University, Wellington 6012, New Zealand

[§]Biomolecular Interaction Center, University of Canterbury, Christchurch 8140, New Zealand

ABSTRACT: Low-molecular-weight organic molecules, such as coumarins and stilbenes, are used commercially as fluorescent whitening agents (FWAs) to mask photoyellowing and to brighten colors in fabrics. FWAs achieve this by radiating extra blue light, thus changing the hue and also adding to the brightness. However, organic FWAs can rapidly photodegrade in the presence of ultraviolet (UV) radiation, exacerbating the yellowing process through a reaction involving singlet oxygen species. Inorganic nanoparticles, on the other hand, can provide a similar brightening effect with the added advantage of photostability. We report a targeted approach in designing new inorganic silicon- and germanium-based nanoparticles, functionalized with hydrophilic (amine) surface terminations as novel inorganic FWAs. When applied on wool, by incorporation in a sol−gel Si matrix, the inorganic FWAs improved brightness properties, demonstrated enhanced photostability toward UV radiation, especially the germanium nanoparticles, and also generated considerably lower levels of reactive oxygen species compared to a commercial stilbene-based organic FWA, Uvitex NFW.

KEYWORDS: *Silicon, germanium, nanoparticles, FWA, fiber, wool*

INTRODUCTION

Natural and synthetic organic molecules undergo photodegradation upon exposure to sunlight in the presence of oxygen. For proteinaceous materials, such as silk and wool, irradiation at wavelengths less than 380 nm can cause photoyellowing via the formation of highly colored species, while wavelengths greater than 380 nm can result in photobleaching.[1−3] Fluorescent whitening agents (FWAs), also called optical brightening agents, are used as additives to brighten colors and mask natural yellowing.[4] FWAs preferentially absorb ultraviolet (UV) radiation in the 360−380 nm wavelength region and re-emit a portion of this as longer wavelength visible light on the blue side of the spectrum, mainly in the region of 400−500 nm.[5] This causes treated materials to reflect a greater proportion of visible light, notably in the blue range, making it appear brighter.[5]

Off-white fiber and fabric treated with FWAs can appear both whiter and brighter when observed under daylight or an illumination source with an appreciable amount of UV light around the 350 nm range. FWAs act by radiating extra blue light, thus changing the hue away from yellow or brown toward white. The effect of FWAs can thus be compared to that of blue dyes and pigments that are often used in the textile and laundry industries to produce a bluish gray tint. FWAs, however, radiate more reflected energy in the form of violet, blue, or greenish color, also adding to the brightness of the fabric.[4]

Current commercial brightening agents are based around organic compounds, including stilbenes and coumarins. Although producing an initial intense brightening effect, these organic additives are photodegraded relatively quickly, with their products thought to contribute to fabric yellowing.[6,7] In addition, the UV-induced photoyellowing of protein-based textiles can be exacerbated by organic FWAs through photosensitization.[2] Singlet oxygen formed by the reaction of ground-state molecular oxygen with FWAs can react with susceptible amino acid residues in wool, particularly methionine, histidine, and tryptophan, with the resulting colored products contributing to the photoyellowing process.[3]

Inorganic nanoparticles can be tailored to absorb strongly in the UV region and to emit blue light and can fluoresce with high quantum yield when attached to solid substrates.[8,9] Such nanoparticles provide a potential route to a new class of fiber whitening agents with enhanced color and photostability properties. We present here a targeted approach to the design of new silicon- and germanium-based nanoparticles and evaluate their performance as FWAs when applied to wool fabric through incorporation into a sol−gel surface treatment.

MATERIALS AND METHODS

Materials. Anhydrous hexane, germanium chloride ($GeCl_4$), tetrachlorosilane ($SiCl_4$), chloroplatinic acid (H_2PtCl_6), lithium borohydride ($LiBH_4$), anhydrous isopropanol, allylamine, luminol, aminopthalic acid, rose bengal, tetraethoxysilane, phenyltriethoxysilane, (3-glycidyloxypropyl)trimethoxysilane, hexadecyltrimethoxysilane, and propylene glycol propyl ether (DOWANOL PnP) were obtained from Sigma-Aldrich Chemicals (St. Louis, MO). Pentaethylene glycol monododecyl ether ($C_{12}E_5$), a non-ionic surfactant, was from Nikko Chemicals Co., Tokyo, Japan, and Uvitex NFW [4,4′-bis(2-sulfostyryl)biphenyl (DSBP)] was from BASF. All other chemicals were also of analytical grade.

Received: January 9, 2013
Revised: June 30, 2013
Accepted: July 4, 2013
Published: July 4, 2013

Clean plain-woven undyed merino wool fabric with a unit weight of 138 g/m^3 was used in this study. Crossbred semi-worsted wool with an average diameter of 42 μm was used to make the fabric.

Methods. *Nanoparticle Synthesis.* In a typical synthesis, 100 mL of anhydrous hexane was added to a three-necked flask attached to a Schlenk line and purged with nitrogen. The surfactant, $C_{12}E_5$, and precursors, $GeCl_4$ or $SiCl_4$, were removed from the glovebox in airtight syringes and injected into the reaction flask. Hydrogen-terminated Si and Ge nanoparticles were then formed by adding a stoichiometric amount of $LiBH_4$ as a reducing agent. After the above mixture was reacted for 2 h, 2 mL of allylamine was added to modify the surface of the nanoparticles. H_2PtCl_6 in isopropanol was used as a catalyst. The nanoparticles were then purified by first removing the hexane by rotary evaporation and subsequently filtered. The filtrate was then concentrated to about 1 mL and applied to a 1 cm diameter Sephadex LH-20 column (bead size of 25−100 μm) (Sigma-Aldrich Chemicals, St. Louis, MO) and eluted with methanol. The flow rate was 1 drop/5 s, with fractions being collected every 50 drops. Each fraction was checked for luminescence in a RPR-600 photochemical mini reactor at 365 nm (Rayonet, Branford, CT). The luminescent fraction was then collected and concentrated to 1 mL to yield surface-modified Si and Ge nanoparticles.[10]

Fluorescence Evaluation. Photoluminescence spectra were obtained using a J-Y Fluorolog fluorescence spectrometer, with a 5 mm slit width in both emission and excitation.

Irradiation. Irradiation was performed in a UV chamber (Luzchem Research, Inc., Ottawa, Ontario, Canada) using UVA (Hitachi FL8BL-B, 300−400 nm) and UVB (Luzchem LZC-UVB, 280−315 nm) lamps. The samples were irradiated over periods of 24 or 48 h for UVA and 12 or 24 h for UVB. The UVA and UVB dosages obtained from the irradiation chamber used in this study were 52.7 and 35.3 W/m^2, respectively.

Reactive Oxygen Species (ROS) Generation Assay. High-performance liquid chromatography (HPLC) assays for the determination of the production of ROS (mainly singlet oxygen species)[11] by FWAs were performed as follows: An Ultimate 3000 system (Dionex Corporation, Sunnyvale, CA) equipped with a 250 × 4.6 mm inner diameter Hi-Pore RP-304 reversed-phase column (Bio-Rad Laboratories, Inc., Hercules, CA), along with a guard column, was used for this assay. An isocratic mobile phase containing acetonitrile and Na_2HPO_4 buffer (0.033 mol/L, pH 8) in the ratio of 7:15 was used at a flow rate of 0.5 mL/min. The eluants were monitored at 351 nm. The analysis was performed at 22 °C, and an equilibration time of 10 min was used between runs. Solutions of 1 mM luminol were analyzed before and after irradiation with or without the addition of 0.2 mM rose bengal, 0.25 mM Uvitex NFW, 0.3 μM amine-capped Si amine, and 0.3 μM amine-capped Ge amine.

Surface Matrix Preparation and Application. As a means of evenly dispersing the nanoparticles on wool fabric samples, a sol−gel Si matrix was prepared. A total of 15 mL of ethanol was mixed with 6.4 mL of tetraethoxysilane, 3.8 mL of phenyltriethoxysilane, 1.2 mL of (3-glycidyloxypropyl) trimethoxysilane, and 0.75 mL of hexadecyltrimethoxysilane. HCl (3.6 mL, 0.01 N) was added dropwise to the solution and stirred for 24 h at room temperature. The sol−gel was 90% diluted in 3:1 water/DOWANOL PnP (3:1, v/v). Nanoparticles were dispersed in the sol−gel at a concentration of ~2.106 × 10^{15} particles/mL using an ultrasonication bath for 2 min. Wool fabric samples (6 × 6 cm) were treated with the sol−gel with or without incorporated nanoparticles by dip-coating for 5 min. The coated fabrics were dried overnight at room temperature and were annealed for 1 h at 120 °C.

Color Measurement. All data were recorded using D65 2 Deg (Illu/Obs). Color measurements before and after UV irradiation were taken using a Chroma Meter CR210 (Minolta, Japan), with a wide area illumination, a 2° viewing angle, and a 50 mm diameter measuring area to average the reading over a wide area, which is suitable for measuring cloth or textured surfaces. Each color measurement represents the average of three readings.

Scanning Electron Microscopy (SEM). SEM images were taken from both untreated and treated fabric samples to evaluate any changes in the surface morphology. The SEM images were collected by mounting the samples onto an aluminum slide using conductive carbon adhesive tape. The samples were sputter-coated from a gold/palladium source and studied using a JEOL JSM 7000F field emission gun scanning electron microscope (Tokyo, Japan). The microscope was operated at 5.0 kV, and samples were viewed at a working distance of 15 mm.

Scanning Transmission Electron Microscopy Energy-Dispersive Spectroscopy (STEM−EDS). The chemical composition of the FWA were investigated by STEM−EDS mapping using a JEOL 2010 transmission electron microscope. Samples were embedded in an Araldite epoxy resin before being cut into thin films using an ultramicrotome and were then placed on a holey carbon grid for electron microscopy analysis.[12]

Abrasion Testing. Abrasion resistance was measured using a Martindale fabric abrasion tester according to the WNZ TM 112 1994 test method.[13] Fabric samples with various treatments were mounted with foam, and a pressure of 9 kPa was applied. These were then subjected to 500 rubs in the form of a geometric figure against a standard wool abradant SM25.

RESULTS AND DISCUSSION

Surface-Functionalized Nanoparticles. Both Si and Ge nanoparticles exhibit low photoluminescence efficiencies in the bulk, [14] but when the diameter of the crystal is reduced to less than the Bohr radius, quantum confinement (a change of electronic and optical properties when the material is of sufficiently small size) increases the probability of radiative recombinations via direct bandgap transitions, leading to enhanced photoluminescence efficiency in the visible region.[14,15] This requires the physical dimensions of the nanoparticles to be in the order of or less than the bulk excitation Bohr radius: 4 nm for Si and 11.5 nm for Ge.[8,9,15−18] The larger excitonic Bohr radius implies that Ge nanoparticles will exhibit stronger effects of quantum confinement than Si nanoparticles of the same size. Ge nanoparticles were thus expected to exhibit photoluminescence in the visible wavelength region with higher quantum yields than Si nanoparticles.

Si and Ge nanoparicles were synthesized for this study with a particle size of approximately 2.5 ± 0.5 and 5 ± 0.5 nm, respectively, and were functionalized with hydrophilic (amine) surface terminations. By optimizing the reaction conditions, monodisperse silicon and germanium nanoparticles of uniform size were produced, thus giving rise to sharp blue photoluminescence in the visible region.

Fluorescence Measurements of Nanoparticles in Dispersion. Fluorescence measurements were conducted by dispersing nanoparticles in ethanol using ultransonication. Photoluminescence measurements were conducted using a spectrofluorometer at an excitation of 400 nm. Both Ge and Si nanoparticles had similar emission maxima at around 475 nm (Table 1).

Dry State Fluorescence of Nanoparticles. For apparel textile applications, it is important that any potential bright-

Table 1. Emission Peaks Obtained at an Excitation of 400 nm of FWA Coated on Fabric Pieces

sample	dispersed in ethanol (nm)	dispersed in Si matrix (nm)	as a fabric coating (nm)
Ge amine	460	425	468
Si amine	475	425	475
Uvitex NFW	460	525	430
Si matrix	no fluorescence	no fluorescence	no fluorescence

dx.doi.org/10.1021/jf401464r | J. Agric. Food Chem. 2013, 61, 7188−7194

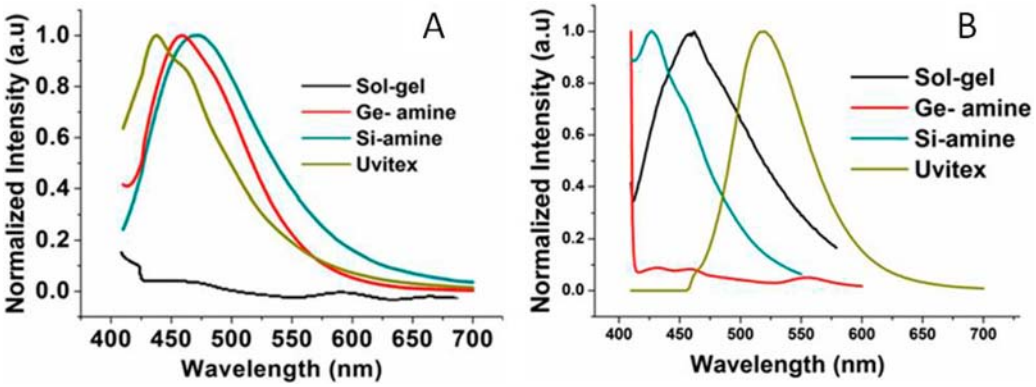

Figure 1. (A) Dry state photoluminescence spectra of Si and Ge nanoparticle FWAs, the organic FWA (Uvitex NFW), and Si matrix sol−gel with 400 nm excitation and (B) emission spectrum of FWAs dispersed in Si matrix sol−gel (excitation at 400 nm).

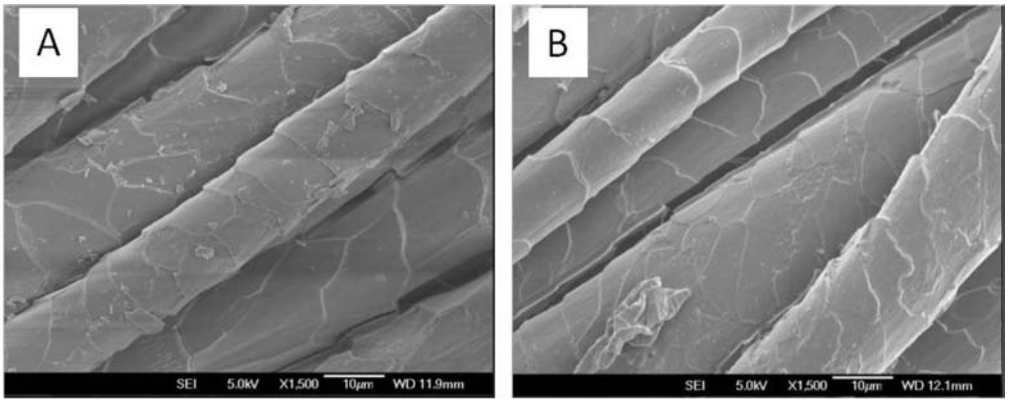

Figure 2. SEM images (1500×) of Si-matrix-coated fabric with (A) Ge amine nanoparticles and (B) Si amine nanoparticles.

ening agents perform well in the dry (non-aqueous) state. Accordingly, prior to fabric treatments, an evaluation of the dry state fluorescence properties of the Si and Ge amines was performed, as shown in Figure 1A and contrasted with a commercially available FWA, Uvitex NFW. Thin films of nanoparticles were obtained by coating a glass slide with the nanoparticles dispersed in ethanol followed by air drying at ambient temperature. The nanoparticles displayed intense blue light emission at 400 nm excitation, with emission maxima ranging between 468 and 475 nm, confirming that their brightening properties are maintained in the dry state (in comparison to solution-state fluorescence in Table 1).

Nanoparticle Fluorescence Dispersed in Si Matrix (Sol−Gel). Photoluminescence measurements of the nanoparticles dispersed in a Si matrix sol−gel were also taken (Figure 1B). Excitation at 400 nm in the presence of the Si matrix (Figure 1B) caused the emission maxima of the nanoparticles to shift to shorter wavelengths, in the violet−blue region of the visible spectrum. The commercial FWA, Uvitex NFW, emitted at a longer wavelength of 525 nm and was thus in the green region of the visible spectrum. Because a violet−blue emission for fluorescent whitening agents is more desirable compared to green, to compensate for fiber yellowing, the general emission profile of the nanoparticles dispersed in the Si matrix appears to be more favorable than Uvitex NFW for material brightening applications.

Nanoparticle Fluorescence When Applied as a Fabric Coating. Emission scans were also obtained for fabric pieces coated with nanoparticles incorporated into a Si matrix sol−gel. The coated fabric pieces were excited at 400 nm, and the emission peaks obtained are shown in Table 1. Fabric pieces with only the Si matrix coating remained non-fluorescent. When inorganic nanoparticle FWAs were incorporated into the Si matrix, the fabrics displayed emission maxima between 468 to 475 nm, similar to the maxima observed for the nanoparticles in dispersion (Table 1). The emission range of the inorganic nanoparticles was more centralized in the blue region of the visible range. The emission maximum of the fabric treated with the organic FWA, Uvitex NFW, however shifted closer to the near UV range, as observed in its dry state (Figure 1A). If the fluorescence resulting from a FWA is partly within the invisible UV range, this can potentially decrease the overall perceived luminance of the treated fabric. The emission properties of the nanoparticles are therefore more suited to improving the brightness properties of fabric than Uvitex NFW. These results demonstrate that inorganic nanoparticles possess fluorescence emission properties well-suited for use as commercial FWAs for fabrics.

SEM of Coated Fabric. SEM images taken of fabric samples before and after coating with the matrix and with the nanoparticles incorporated in the matrix demonstrated a reasonably good surface coverage. The matrix coating alone did not show any obvious cracks when observed at the higher magnifications. However, when nanoparticle or Uvitex NFW FWAs were added to the matrix, a slight patchiness of the coating was observed. The coating did not completely obscure scale definition with no observable detachment of the matrix from the fiber surface, indicating a thin (desirable) distribution of the coating on the fiber surface (Figure 2).

STEM−EDS of Nanoparticle-Coated Fabric. Because the sol−gel matrix itself contains silicon, an EDS map of silicon nanoparticle-coated fibers would prove futile. Germanium-nanoparticle-coated fabrics were therefore only used in this study. Figure 3A is a transmission electron microscopy (TEM) image of a section of germanium-1-hexene-coated wool fabric. Panels B, E, and F of Figure 3 are EDS maps (carbon, sulfur, and oxygen, respectively) of the wool fiber representing the basic elements that constitute wool. Silicon in Figure 3C is from the sol−gel matrix, while germanium (Figure 3D) is from the nanoparticle coating in the fiber. Because the silicon image closely matches the germanium image, it can be inferred that a uniform distribution of the germanium nanoparticles within the sol−gel was obtained.

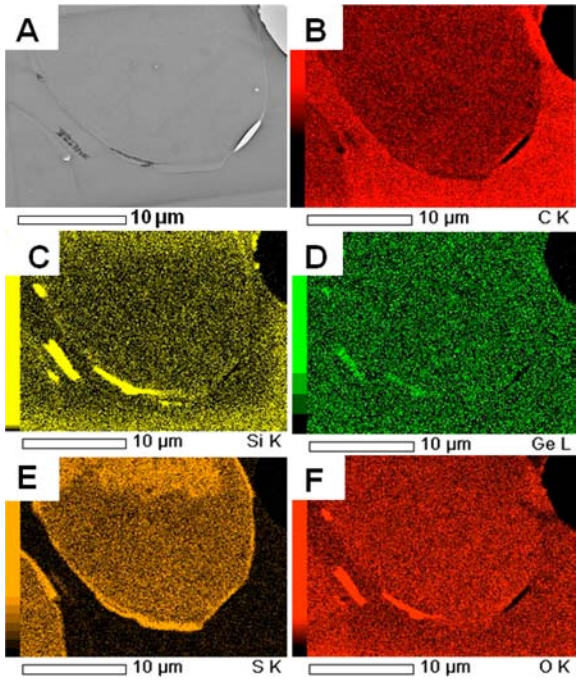

Figure 3. (A) TEM image of a section of Ge-amine-nanoparticle-coated fabric. EDS maps showing the distribution of (B) carbon, (C) silicon, (D) germanium, (E) sulfur, and (F) oxygen in the coated fabric.

Abrasion Test. Measurement of textile resistance to abrasion is very complex and can be affected by many factors, such as the dimensions and inherent mechanical and structural properties of the fibers, the construction of the fabrics, and the type, kind, and amount of finishing material added to the fibers, yarns, or fabrics.[13] The response of the fabrics to abrasion was assessed by imaging with SEM (Panels A−C of Figure 4). Severe loss of edge definition of the cuticle layer along with some cuticle separation was observed in the control sample, which did not have any treatment. This indicated a loss of the cuticle layer and possible exposure of the endocuticle (Figure 4A). Matrix application provided a degree of resistance against abrasion. Abrasion resistance with Si (Figure 4B) and Ge (Figure 4C) nanoparticles embedded in the matrix was satisfactory, with the highest abrasion resistance observed for the Ge-nanoparticle-embedded matrix coating, where cuticular edge definition was well-preserved.

Brightening Effect. To compare the brightening effect of the nanoparticles with Uvitex NFW, squares of matrix-treated wool fabric impregnated with either Uvitex NFW or inorganic nanoparticles were exposed to both UVA and UVB radiation, and the CIE *Y* values were recorded. *Y* relates to the perception of lightness, and therefore, an increase in the *Y* value indicates an increase in brightness of the sample. Each color measurement represents the average of three readings from three separate samples. The brightness of the nanoparticle-treated samples and those treated with Uvitex NFW was recorded. The *Y* values of fabrics exposed to UVA and UVB radiation along with their standard errors of the mean are displayed in Figure 5.

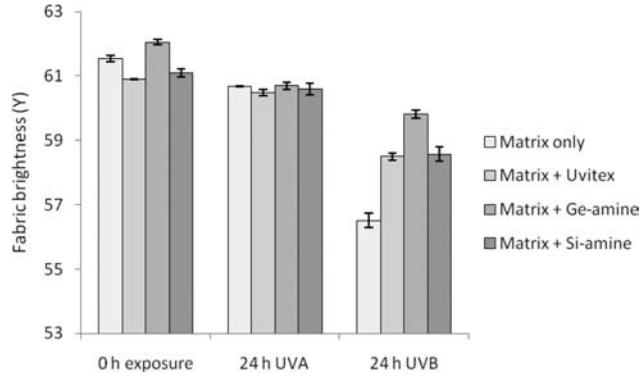

Figure 5. *Y* (brightness) fabric scores before and after 24 h of UVA and UVB irradiation, with Ge amine and Si amine nanoparticles (~2.106×10^{15} particles/mL) and Uvitex NFW (0.2 mM) dispersed in the Si matrix.

The matrix-only-treated wool fabric samples initially appeared brighter than either the Uvitex NFW or Si-amine-treated samples. However, Ge-amine treatments resulted in the brightest fabrics (Figure 5). UVA radiation for 24 h decreased the brightness level of all four treatments to a similar level

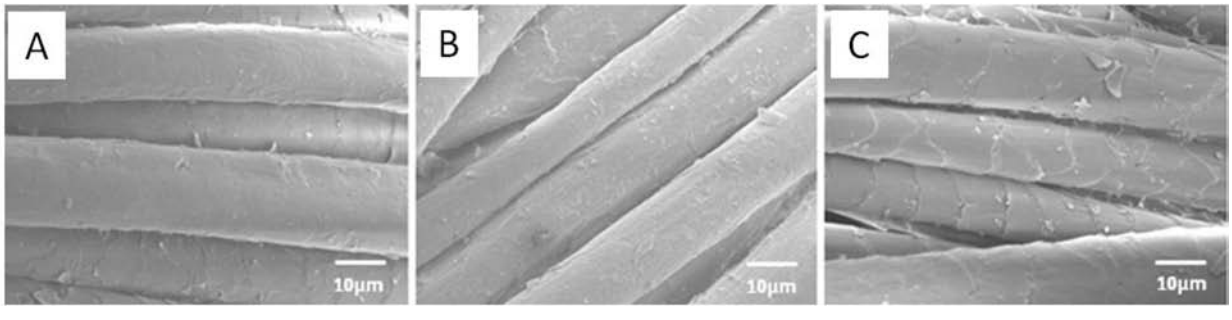

Figure 4. SEM images (1500×) showing the response to abrasion test of (A) control wool fabric without any coating, (B) wool fabric coated with Si amine dispersed in Si matrix, and (C) wool fabric coated with Ge amine dispersed in Si matrix.

dx.doi.org/10.1021/jf401464r | J. Agric. Food Chem. 2013, 61, 7188−7194

(Figure 5). The biggest difference as a result of treatment was observed upon exposure to UVB radiation. The brightness of the fabrics treated with matrix only was reduced significantly, with smaller reductions in brightess for Uvitex-NFW- and Si-amine-treated samples. The Ge amine treatment clearly improved the retention of fabric brightness during UVB exposure (Figure 5).

While initial brightening is a desirable feature of FWAs, more importantly, they must display stability over the product life of a treated fabric. Ideally, FWAs should not be readily discolored or destroyed by light or even chemicals used in laundering. The brightness stability of the fabric pieces treated with Uvitex NFW and the nanoparticles is shown in Figure 6 for both UVA and UVB.

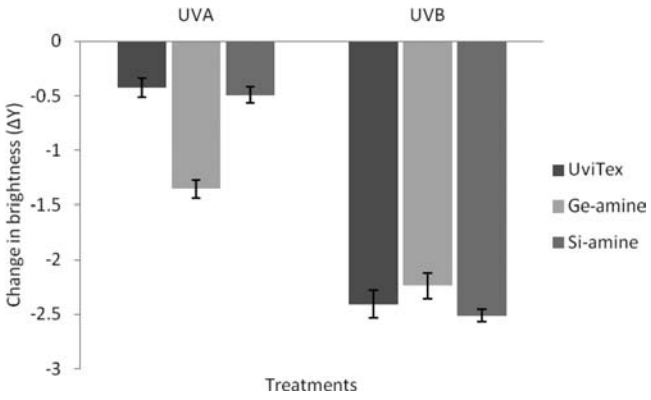

Figure 6. ΔY (loss of brightness) in fabric samples after 24 h of UVA and UVB irradiation.

All of the samples decreased in brightness after UVA and UVB exposure. Si-amine- and Uvitex-NFW-treated samples displayed similar small losses of brightness, while Ge amine treatment resulted in a slightly larger loss of brightness upon exposure to UVA radiation. However, the decreases in brightness were not significant between treatments, indicating that these treatments possess similar stability toward UVA radiation. Upon exposure to 24 h of UVB radiation, all three treatments decreased similarly in brightness, to a greater extent than after UVA exposure.

Fabric exposed to UVA or UVB irradiation may undergo both photoyellowing and photobleaching, because of the formation and subsequent destruction of protein-derived chromophores. Hence, it is also important that the FWAs do not exacerbate such reactions by generating free radicals in the presence of UV radiation. A disadvantage of some FWAs is that they can decompose, forming yellow products, or act as photosensitizers of protein degradation by forming highly reactive intermediates.[19,20] Measuring fabric yellowness using CIE $Y-Z$ is a means of assessing the level of photoyellowing occurring as a consequence of treatment. The initial $Y-Z$ values of Uvitex-NFW-, Si-amine-, and Ge-amine-treated fabrics were very similar to each other (Uvitex NFW, 11.52 ± 0.38; Ge amine, 11.47 ± 0.13; and Si amine, 11.79 ± 0.76). To determine the change as a result of photoyellowing, the change in $Y-Z$ values ($\Delta Y-Z$) after UV exposure was recorded for the Uvitex NFW, Si amine, and Ge amine samples. The difference in color stability of the nanoparticle-treated fabrics relative to that of Uvitex-NFW-treated fabrics was measured with Uvitex NFW relative color stability defined as zero. The level of photoyellowing following Ge amine treatment was similar to that following Uvitex NFW treatment upon exposure to 24 h of UVA radiation (0.07 ± 0.04). Si-amine-treated fabric, however, photoyellowed considerably less than Uvitex-NFW-treated fabric during UVA exposure (−0.70 ± 0.40). Following UVB exposure, both Ge amine and Si amine treatments provided better photoprotection than Uvitex NFW treatment. The greatest level of protection was conferred by Ge amine (−0.72 ± 0.41) followed by Si amine (−0.42 ± 0.25). The improvement demonstrated by Ge amine treatment may be due to its blue fluorescence canceling out the photoyellowing effect of UV radiation, or it could be that, at the concentration used to coat the fabric pieces, the decomposition of the nanoparticles is quite low, whereas organic FWAs, such as Uvitex NFW, may degrade to colored species.[6,7] Another reason, which would be highly desirable, is that, because of their inorganic nature, these nanoparticles do not act as photosensitizers, unlike organic FWAs and, hence, do not induce residue modifications leading to proteinaceous photoyellowing.

For the UVA irradiation, a 24 h exposure was equivalent to approximately 1−2 years of regular sunlight exposure through window glass.[21,22] The photostability of fabrics under our irradiation conditions therefore represents a good correspondence to the color stability that can be achieved by these treatments in terms of real product life.

Overall, Ge amine treatment demonstrated satisfactory photostability, brightening, and improved performance in comparison to a currently commercially available organic FWA, Uvitex NFW. Both of these attributes, brightening and photoprotection, are desirable features of high value fibers and textiles. These results demonstrate the potential for inorganic FWAs to match or exceed the performance of current organic FWA while potentially offering other advantages, such as lowered ecotoxicity. The synthesis of silicon and germanium nanoparticles can be achieved via several economically viable methods, making the high-value fibers and textiles of great potential economic interest.[23]

ROS Generation. ROS are known to be generated by organic FWAs under UV irradiation, thereby exacerbating the photoyellowing process in wool and other protein-based fibers. At high concentrations, nanoparticles are also reported to generate ROS.[24] The generation of singlet oxygen is known to photosensitize wool through the formation of highly reactive intermediates.[20,25] Here, an assay was adapted to evaluate the levels of singlet oxygen generated by the inorganic silicon nanoparticles, with correlation to the levels generated by the reference stilbene-based organic FWA, Uvitex NFW.

This HPLC assay is based on monitoring singlet oxygen generation via the degradation of luminol to aminopthalic acid.[11] Oxidative decomposition of luminol was monitored in the presence of the inorganic nanoparticles, rose bengal (a well-known photosensitizer),[11] and Uvitex NFW, before and after exposure to 1, 6, and 12 h of UV irradiation.

The control assay demonstrated the formation of aminopthalic acid as a result of photo-oxidation of luminol, with almost total degradation of luminol after 12 h of UVA irradiation. As anticipated, the singlet oxygen generator, rose bengal, exacerbated luminol degradation upon UVA exposure, with considerable degradation after only 1 h of irradiation. In the presence of Uvitex NFW, significant degradation of luminol to aminopthalic acid was observed after 6 h of UVA irradiation. luminol degradation by singlet oxygen during UVA irradiation was also observed in the presence of high concentrations (6.318 × 10^{15} particles/mL) of the inorganic Si amine and Ge amine

nanoparticles (Table 2). However, for longer UVA exposure times of 12 h, luminol degradation in the presence of Uvitex NFW, although lower than that with Si amine nanoparticles, was considerably higher than that with the Ge amine nanoparticles. Over 12 h, 91% of the luminol degraded to aminopthalic acid in the presence of Uvitex NFW and more than the 85% of the luminol degraded to aminopthalic acid in the presence of Ge amine nanoparticles. As measured by luminol degradation, the Ge amine generated the least singlet oxygen.

Table 2. Percent Degradation of Luminol on UVA Exposure in the Presence of Si and Ge Nanopaticles and Uvitex NFW

	degradation of luminol		
sample	1 h of UVA (%)	6 h of UVA (%)	12 h of UVA (%)
Ge amine (0.3 μM)	13	90	91
Si amine (0.3 μM)	29	86	94
Uvitex NFW (0.25 mM)	17	84	85

The results from this study demonstrated that tailored silicon- and germanium-based nanoparticles, surface-modified with allylamine, performed as FWAs when applied to wool fabric by incorporation in a sol−gel surface treatment. In comparison to Uvitex NFW, the brightness conferred to fabrics treated with either germanium or silicon nanoparticles demonstrated improved brightness during exposure to either UVA or UVB irradiation. Both Si amine and Uvitex NFW were more photostable compared to Ge amine in the presence of UVA, but in the presence of UVB, Ge amine demonstrated the highest photostability. When the stability of treated fabrics to photoyellowing was investigated, Si amine treatments provided superior photoprotection against UVA, while Ge amine treatments provided superior photoprotection against UVB. The nanoparticles displayed an emission maxima in the blue region of the visible spectrum, suited to improving fabric brightness properties. When incorporated in a sol−gel matrix and applied onto fabric, surface distribution was acceptable. Because of these favorable properties, these inorganic nanoparticles are demonstrated to be well-suited for use as commercial FWAs for fabrics, with enhanced performance compared to currently used organic FWAs, while potentially also offering added advantages, such as lowered ecotoxicity.

AUTHOR INFORMATION

Corresponding Author

*Telephone: +64-3-321-8758. Fax: +64-3-321-8811. E-mail: santanu.deb-choudhury@agresearch.co.nz.

Funding

Funding for this project was provided by Australian woolgrowers and the Australian Government through Australian Wool Innovation Limited (AWI). Richard D. Tilley and Sujay Prabakar thank the MacDiarmid Institute for funding and the Ministry of Science and Innovation (MSI) for funding through Grant PROP-20106-ICE-MAU.

Notes

The authors declare no competing financial interest.

ACKNOWLEDGMENTS

We gratefully acknowledge the assistance of Dr. Anita Grosvenor for technical editing of this manuscript.

ABBREVIATIONS USED

FWA, fluorescent whitening agent; TEM, transmission electron microscopy; SEM, scanning electron microscopy; STEM−EDS, scanning transmission electron microscopy energy-dispersive spectroscopy

REFERENCES

(1) Davidson, R. S. The photodegradation of some naturally occurring polymers. *J. Photochem. Photobiol., B* **1996**, *33*, 3−25.

(2) Dyer, J. M.; Bringans, S. D.; Bryson, W. G. Determination of photo-oxidation products within photoyellowed bleached wool proteins. *J. Photochem. Photobiol.* **2006**, *82*, 551−557.

(3) Dyer, J. M.; Bringans, S. D.; Bryson, W. G. Characterisation of photo-oxidation products within photoyellowed wool proteins: Tryptophan and tyrosine derived chromophores. *J. Photochem. Photobiol. Sci.* **2006**, *5*, 698−706.

(4) Kramer, J. B.; Canonica, S.; Hoigné, J.; Kaschig, J. Degradation of fluorescent whitening agents in sunlit natural waters. *Environ. Sci. Technol.* **1996**, *30*, 2227−2234.

(5) Millington, K. R. Improving the photostability of whitened wool by applying an anti-oxidant and metal chelator rinse. *Color. Technol.* **2006**, *122*, 49−56.

(6) Dyer, J. M.; Cornellison, C. D.; Bringans, S. D.; Maurdev, G.; Millington, K. R. The photoyellowing of stilbene-derived fluorescent whitening agents—Mass spectrometric characterization of yellow photoproducts. *J. Photochem. Photobiol.* **2008**, *84*, 145−153.

(7) Davidson, R. S.; Ismail, G. M.; Lewis, D. M. The photosensitising properties and photostability of stilbene fluorescent whitening agents. *J. Soc. Dyers Colour.* **1987**, *103*, 261−264.

(8) Tilley, R. D.; Warner, J. H.; Yamamoto, K.; Matsui, I.; Fujimori, H. Micro-emulsion synthesis of monodisperse surface stabilized silicon nanocrystals. *Chem. Commun.* **2005**, 1833−1835.

(9) Warner, J. H.; Hoshino, A.; Yamamoto, K.; Tilley, R. D. Water-soluble photoluminescent silicon quantum dots. *Angew. Chem., Int. Ed.* **2005**, *44*, 4550−4554.

(10) Prabakar, S.; Shiohara, A.; Hanada, S.; Fujioka, K.; Yamamoto, K.; Tilley, R. D. Size controlled synthesis of germanium nanocrystals by hydride reducing agents and their biological applications. *Chem. Mater.* **2010**, *22*, 482−486.

(11) Wierrani, F.; Kubin, A.; Loew, H. G.; Henry, M.; Spängler, B.; Bodner, K.; Grünberger, W.; Ebermann, R.; Alth, G. Photodynamic action of some sensitizers by photooxidation of luminol. *Naturwissenschaften* **2002**, *89*, 466−469.

(12) Glauert, A. M.; Glauert, R. H. Araldite as an embedding medium for electron microscopy. *J. Biophys. Biochem. Cytol.* **1958**, *4*, 191−194.

(13) ASTM International. *ASTM D4158-08 Standard Guide for Abrasion Resistance of Textile Fabrics (Uniform Abrasion)*; ASTM International: West Conshohocken, PA, 2012; http://www.astm.org/Standards/D4158.htm.

(14) Holmes, J. D.; Ziegler, K. J.; Doty, R. C.; Pell, L. E.; Johnston, K. P.; Korgel, B. A. Highly luminescent silicon nanocrystals with discrete optical transitions. *J. Am. Chem. Soc.* **2001**, *123*, 3743−3748.

(15) Tilley, R. D.; Yamamoto, K. The microemulsion synthesis of hydrophobic and hydrophilic silicon nanocrystals. *Adv. Mater.* **2006**, *18*, 2053−2056.

(16) Warner, J. H.; Tilley, R. D. Synthesis of water-soluble photoluminescent germanium nanocrystals. *Nanotechnology* **2006**, *17*, 3745−3749.

(17) Shiohara, A.; Prabakar, S.; Faramus, A.; Hsu, C.-Y.; Lai, P.-S.; Northcote, P. T.; Tilley, R. D. Sized controlled synthesis, purification, and cell studies with silicon quantum dots. *Nanoscale* **2011**, *3*, 3364−3370.

(18) Shiohara, A.; Hanada, S.; Prabakar, S.; Lim, T. H.; Fujioka, K.; Yamamoto, K.; Northcote, P. T.; Tilley, R. D. Chemical reactions on surface molecules attached to silicon quantum dots. *J. Am. Chem. Soc.* **2010**, *132*, 248−253.

(19) Millington, K. R.; Maurdev, G. The generation of superoxide and hydrogen peroxide by exposure of fluorescent whitening agents to

UVA radiation and its relevance to the rapid photoyellowing of whitened wool. *J. Photochem. Photobiol., A* **2004**, *165*, 177−185.
(20) Davidson, R. S.; Ismail, G. M.; Lewis, D. M. Retardation of the photoyellowing of untreated wool and wool treated with fluorescent whitening agents by the action of reducing agents. *J. Soc. Dyers Colour.* **1987**, *103*, 308−313.
(21) Chadysiene, R.; Girgzdiene, R.; Girzdys, A. Ultraviolet radiation and ground-level ozone variation in Lithuania. *J. Environ. Eng. Landscape Manage.* **2005**, *13*, 31−36.
(22) Giampieri, F.; Alvarez-Suarez, J. M.; Tulipani, S.; González Paramás, A. M.; Santos-Buelga, C.; Bompadre, S.; Quiles, J. L.; Mezzetti, B.; Battino, M. Photoprotective potential of strawberry (*Fragaria* × *ananassa*) extract against UV-A irradiation damage on human fibroblasts. *J. Agric. Food Chem.* **2012**, *60*, 2322−2327.
(23) Dasog, M.; Yang, Z.; Regli, S.; Atkins, T. M.; Faramus, A.; Singh, M. P.; Muthuswamy, E.; Kauzlarich, S. M; Tilley, R. D.; Veinot, J. G. C. Chemical insight into the origin of red and blue photoluminescence arising from freestanding silicon nanocrystals. *ACS Nano* **2013**, *7*, 2676−2685.
(24) Fujioka, K.; Hiruoka, M.; Sato, K.; Manabe, M.; Miyasaka, R.; Hanada, S.; Hoshino, A.; Tilley, R.; Manome, Y.; Hirakuri, K.; Yamamoto, K. Luminescent passive-oxidised silicon quantum dots as biological staining labels and their cytotoxicity effects at high concentration. *Nanotechnology* **2008**, *19*, 1−7.
(25) Auer, P. D.; Pailthorpe, M. T. Effect of topical applications of antioxidants and quenchers on the photoyellowing of fluorescently whitened wool fabric. *Text. Res. J.* **1995**, *65*, 287−293.